Liu, Guodong; Maloney, Thaddeus; Dimic-Misic, Katarina; Gane, Patrick

Acid dissociation of surface bound water on cellulose nanofibrils in aqueous micro nanofibrillated cellulose (MNFC) gel revealed by adsorption of calcium carbonate nanoparticles under the application of ultralow shear

Published in:
Cellulose

DOI:
10.1007/s10570-017-1371-1

Published: 01/08/2017

Document Version
Peer-reviewed accepted author manuscript, also known as Final accepted manuscript or Post-print

Acid dissociation of surface bound water on cellulose nanofibrils in aqueous micro nanofibrillated cellulose (MNFC) gel revealed by adsorption of calcium carbonate nanoparticles under the application of ultralow shear

Guodong Liu[1,2], Thaddeus Maloney[1], Katarina Dimic-Misic[1], Patrick Gane[1,3]

[1] School of Chemical Engineering, Department of Bioproducts and Biosystems, Aalto University, FI-00076 Aalto, Helsinki, Finland
[2] College of Bioresources Chemical and Materials Engineering, Shaanxi University of Science and Technology, Xi'an, 710021, China
[3] Omya International AG, Baslerstrasse 42, CH-4665 Oftringen, Switzerland

*Corresponding author: Guodong Liu

E-Mail address: guodong.liu@aalto.fi

Abstract

At ultralow shear rate (~0.01 s^{-1}), acting below the yield stress of the aqueous gel, adsorption of calcium carbonate nanoparticles (<~100 nm) onto cellulose nanofibrils is induced without pigment-pigment preflocculation. Dispersant-free and polyacrylate treated dispersed carbonate particles are compared. Initially, it is seen that the polyacrylate dispersed material does not adsorb, whereas the dispersant-free carbonate adsorbs readily under the controlled ultralow shear conditions. However, repeated cycles of ultralow shear with intermittent periods in the rest state eventually induce the effect as initially seen with the dispersant-free calcium carbonate. The fibril suspension in the bulk is slightly acidic. The addition of buffer to a controlled pH in the case of the dispersant treated particles maintained a similar delay in the onset of adsorption, but adsorption occurred eventually after repeated cycles. During this cycling process, in parallel, the pH gradually drops under repeated cycles of ultralow shear, opposite to expectation, given the buffering capacity of calcium carbonate. The conductivity, in turn, progressively increases slightly at first and then significantly. The action of surface bound water on the nanofibril is considered key to the action of adsorption, and the condition of ultralow shear suggests that the residence time of the particle in contact with the nanofibril, acting under controlled strain against diffusion in the gel, is critical. It is proposed that under these specific conditions the calcium carbonate nanoparticles act as a probe of the nanofibril surface chemistry. The hydrogen bonded water, known to reside at the nanofibril surface, is thus considered the agent in the carbonate-surface interaction, effectively expressing an acid dissociation, and the calcium carbonate nanoparticles act as the probe to reveal it. An important phenomenon associated with this acid dissociation behaviour is that the adsorbed calcium carbonate particles subsequently act to flocculate the otherwise stable cellulose material, leading to release of water held in the aqueous gel matrix structure. This latter effect has major implications for the industrial ease of use of micro and nanofibrillar cellulose at increased solids content. This novel mechanism is also proposed for use to enhance the dewatering capability in general of complex cellulose-containing gel-like water-holding suspensions.

Keywords: micro nanofibrillated cellulose, ultralow shear dewatering/structuration, acid dissociation, cellulose bound water reactivity, ground calcium carbonate, autoflocculation, dewatering mechanism

---

1. Introduction

Environment-friendly and sustainability are crucial targets in industrial application and functional materials, and development of novel biobased composite materials based on renewable sources is considered highly relevant. In the forest bioproducts industry, nanofibrillated (NFC), sometimes referred to as cellulose nanofibres (CNF), and microfibrillated cellulose (MFC) have drawn much attention in the past decades due to their strength giving property potential not only in paper and board manufacturing but also in other industrial value chains, such as nanocomposites [1, 2]. An emerging variant of such fibrillated material is micro nanofibrillated cellulose (MNFC), so-called because it contains a distribution of microfibrils which, in turn, have nanofibrils emanating from their surface formed by mechanical nanofibrillation [3, 4]. This material is chosen because it is endowed with some interesting intrinsic properties, exhibiting particularly high specific surface area, long range structural integrity, regions of internal structural crystallinity and surface chemistry presenting hydroxyl groups for possible chemical modification [2].

In aqueous suspension nanocellulose-containing materials exhibit strong hydrophilicity, and MNFC displays high water absorbency, and, due to the high osmotic pressure within the system, both bound water on the fibril surface and clustered interstitial unbound water are present within the suspension, creating a gel-like material in suspension even at very low consistency (concentration) [5, 6]. Due to their gelation properties, MNFC suspensions are highly water retaining [7, 8]. For some applications extended low shear conditions are necessary where it is favourable that the gel properties are preserved. For these applications, where applied stress is necessarily below the yield stress, any required dewatering must occur within the initially linear viscoelastic region (LVE) [8]. It is this latter question of controlling dewatering which has become a significant area for research. It was seen, for example, that application of ultralow shear below the yield stress in the presence of colloidally-unstable particles, in the form of undispersed precipitated calcium carbonate (PCC), over prolonged time, the free water held in the MNFC gel network could be separated successfully [9]. This effect was attributed to auto-flocculation of the PCC particles under this physical shear condition of ultralow shearing, but what was not known was whether the particles became adsorbed on the fibrils or simply became de-mixed and flocculated [9]. In contrast, polyacrylate dispersed PCC, the dispersant providing the anionic stabilising charge to the dispersed PCC pigment particles, was shown to prevent any autoflocculation or interaction with the similarly charged fibrils under any conditions of applied shear, and thus inhibited the mechanism of water release.

Although the physical states of the fibril-bound versus free gel water have been recently explored in further detail, showing that the bound water is in a restrained state [10, 11], the surface chemical nature of the bound water has not been investigated. The earlier findings, described above in respect to dewatering, indicated that it might be possible to use calcium carbonate as a probe to study the surface activity of the water bound on the fibrils, particularly in respect to any acid moiety, if it could be shown that carbonate nanoparticles might be adsorbed. Following the method of ultralow shearing for dewatering of MNFC by adding PCC particles into suspension, we use similar calcitic fine ground calcium carbonate (GCC), which is widely applied in the paper, board, construction coatings, paints and polymer, water treatment and agriculture industries. Firstly, the findings seen using PCC to induce dewatering under ultralow shear are reproduced using the rhombohedral GCC in both undispersed (UGCC) and polyacrylate dispersed (DGCC) form. Although similar effects could be confirmed contrasting undispersed with dispersed particles as were seen for PCC, by extending the experimental conditions to repeated cycling of ultralow shear with periods of storage, eventually dewatering could also be observed in the case of the dispersed GCC. The eventual destabilisation of the originally dispersed carbonate provides the key to understanding the interaction being developed. Susceptibility to calcium ion dissociation at the calcite surface under weak acidic conditions can lead to calcium chelation via the dispersant until the chelating capacity is saturated. In respect to the buffering capacity of calcite, our study investigates the role of surface bound water on the nanofibrillar component of the MNFC structure in relation to calcium ion dissociation. The balance between particle Brownian motion and the dwell time in contact between GCC particles and the nanofibrils can be extended

by the stress induced when under ultralow shear strain, thus retaining the particle within contact range of the fibril surface against the effects of diffusion.

2. Materials and methods

2.1 MNFC preparation

The MNFC was produced from previously dried bleached birch Kraft pulp from a Finnish pulp mill as the initial material for the pulp preparation, delivering a weighted average fibre length of 1.23 mm measured with a FibreLab analyser (Metso Automation). The pulp was first dispersed for 20 min at 1.8 w/w% solids content (consistency) in a Valley beater without refining. The original pulp of around 300 g was then adjusted to 20 % moisture content with deionised water. It was then subjected to a pretreatment with cellulase enzyme ECOPULP® R (cellulase activity 84 000 $CMUg^{-1}$ determined on CMC-substrate at 60 °C and pH 4.8, as described by the supplier), and the 1.5 mg enzyme per gram of pulp fibre in the pulp suspension was applied to support enzymolysis of the prepared pulp. The pulp was thus hydrolysed at a constant temperature of 55 °C and pH 5.5 for 180 min with a bread mixer under moderate agitation. The resulting suspension was placed in a cold storage to be cooled to less than 4 °C, at which temperature the enzyme was deactivated, and then the material was refined in a Valley Hollander for 30 min and subsequently fed two times through a microfluidiser (model M-110P, Microfluidics, USA) in order to obtain MNFC with favourable particle size and morphology. The pressure in the fluidiser was controlled at 2 000 bar and the flow gap set to 100 um [12]. The pulp was checked after 2 weeks to ensure that the enzyme did not continue the hydrolysis under these conditions, and the effect of the residual enzyme on MNFC properties can therefore be considered negligible. The MNFC was characterised immediately, as shown in Table 1, when it was warmed to room temperature. The solids content of the final MNFC obtained was 21.35 w/w%.

Table 1. The physical properties of the original MNFC

WRV /cm^3g^{-1}	DDJ /%	DCS /$mg.g^{-1}$	sedimentation /cm^3g^{-1}	intrinsic viscosity /cm^3g^{-1}
2.98	11.8	179	10	305

WRV is the swelling water retention value [13], DDJ is the amount of material (fibres) retained on a 200-mesh screen, DSC is the dissolved and colloidal material after centrifuging, sedimentation is the volume of water per gram of MFC after 24 h, intrinsic viscosity is the viscosity of the cellulose by standard techniques.

2.2 Mineral pigments: undispersed (U) and dispersed (D) GCC

The chosen representative pigment material is ground calcium carbonate (GCC) (Covercarb 60-ME: Omya International AG, Baslerstrasse 42, CH-4665 Oftringen, Switzerland) used as typical high light scattering, narrow particle size distribution pigment in paper and board production, produced from Norwegian marble. The dispersed GCC (DGCC) was processed with ~0.01 $g.g^{-1}$ (1 w/w%) of active sodium polyacrylate, displaying 60 w/w% of particles < 1 µm, as defined by equivalent settling diameter in water. GCC is usually dispersed in this way to guarantee the pigment particles remain stable in suspension at elevated solids content (71 w/w%), avoiding flocculation and allowing free Brownian motion between particles, as shown schematically in Fig. 1. The same material, prior to the dispersing process, i.e. in undispersed form (UGCC), is used as a dispersant-free comparative sample, in the form of a thick filtercake suspension material with a solid content of 64 w/w%.

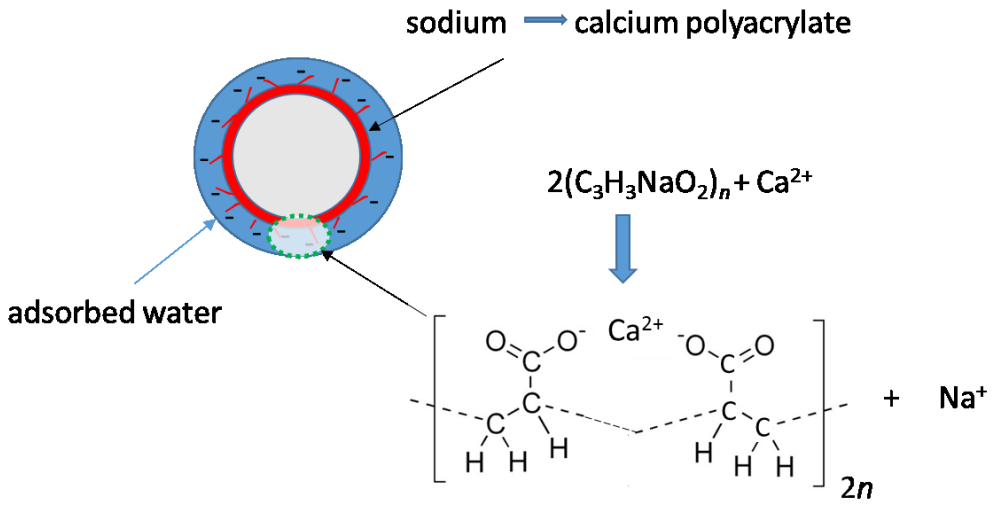

Fig. 1 Schematic of dispersed GCC particle, showing the adsorption of sodium polyacrylate by ion exchange with surface calcium.

2.3 MNFC with UGCC/DGCC composite suspension preparation

5 w/w% MNFC, diluted from the stock MNFC suspension using deionised water, formed an easily mixable suspension, which readily re-establishes a stable gel after mixing. The pigment components were diluted to the same 5 w/w% solids content prior to addition to the MNFC suspension to produce a range of mix ratios MNFC:GCC in parts by weight, namely, 3:7, 4:6, 5:5, 6:4 and 7:3, to form the experimental composite aqueous suspensions, as shown in Table 2.

Table 2. Weight ratios of MNFC and respective GCC pigments

ratio	MNFC:UGCC suspensions			MNFC:DGCC suspensions		
	MNFC (5 w/w%) /g	UGCC (64 w/w%) /g	total weight (5 w/w%) /g	MNFC (5 w/w%) /g	DGCC (71 w/w%) /g	total weight (5 w/w%) /g
3:7	25	4.56	83.33	27	4.44	90.00
4:6	35	4.10	87.50	35	3.70	87.50
5:5	45	3.52	90.00	45	3.17	90.00
6:4	55	2.87	91.67	55	2.58	91.67
7:3	65	2.18	92.86	65	1.96	92.86

2.4 Tris buffer solution

Tris(hydroxymethy) amino-methane, $(HOCH_2)_3CNH_2$ (Sigma-Aldrich, USA, ≥ 99.8 %), was used in certain experiments to establish a start pH and to test control against bulk pH drop. The concentration and pH value of tris buffer solution were set to c = 0.1 mol.dm^{-3} and pH 7.85, respectively.

2.5 Calcium ion (Ca^{2+}) source and weak acid for mechanistic testing

In order to find out the form in which calcium release from the GCC became incorporated in the composite, Ca^{2+} was introduced into the suspension as a control sample by adding $CaCl_2{\cdot}2H_20$ (FF-Chemicals Oy, Finland, ≥ 95 %) at a concentration of 1 % in solution. Weak acid (acetic), CH_3COOH (100 %, w/w, Merck KGaA, 64271 Darmstadt, Germany), was employed in combination with the calcium salt to simulate and explore the structural changes including Ca^{2+} ion release during the experiment as a function of reduced pH in the

suspension. This was achieved in the presence of a weak acid and conjugate base/chelating agent (polyacrylate), creating conditions of so-called acid tolerance, in which the calcium carbonate no longer acts to buffer the suspension (calcite natural pH ~8.5), thus retaining a neutral to acid pH range without dissolution of the GCC [14]. The concentration of CH_3COOH was diluted to 1 %, 5 % and 10 % with deionised water, respectively, before use, so as to avoid acid shock at low concentration, and higher concentration to study the rate of differential flocculation versus adsorption.

2.6 Rheological behaviour using vane in cup geometry

To observe the viscosity changes and the dewatering effect under shear, an ultralow shear rate of 0.01 s^{-1} was applied to the composite suspension samples with vane and cup geometry (Anton Paar Rheometer, Germany): four bladed vane with a diameter of 10 mm and a length of 8.8 mm and a cup with a diameter of 17 mm and a volume of 45 mm^3. In order to ensure consistency, the shearing process was carried out as follows. The sample was mixed and stirred for 30 min. The chosen fixed volume of sample, 33 mm^3, was poured into the cup and gently tapped to remove air bubbles before the gel formation was complete. A uniform level in the cup was maintained for all samples to carry out the rheological tests at 23 °C. All samples were subjected to pre-shearing under medium shear rate (200 s^{-1}) for 5 min, and then let stand for 5 min before applying an ultralow shear of 0.01 s^{-1} for 30 min, during which the viscous response data were collected. The dynamic viscosity is quoted as an average of 3 measurements.

2.7 Observing structure changes with optical microscopy

After applying ultralow shear for an extended period to the composite suspensions, or after controlled storage, changes in the structure in respect to any or all of auto-flocculation of the carbonate, structuration of the fibrillar material, adsorption of carbonate nanoparticles onto the nanofibrils and resulting state of the adsorbed composite were monitored using optical microscopy (LEICA DM 750, Switzerland). Firstly, a clean microscope glass slide was dipped into the suspension and drawn out very slowly, so that a thin layer of liquid suspension was left adhering as a film to the microscope slide. The adhering suspension together with the glass slide was then dried in ambient air, and microscopic images were recorded.

3. Experimental results and discussion

3.1 Free diffusion test for pigments in MNFC suspension

To differentiate and eliminate effects related to auto-flocculation attributed to free diffusion of particles associated with Brownian motion leading to de-mixing from the nanofibrillar cellulose gel, each sample was allowed to stand in a screw-topped plastic sample vial placed on a level surface for 5 h. Only the sample ratio 3:7 of MNFC:UGCC, having the weakest gel structure, showed an approximately 1.5-2 mm water layer separated on its surface due to the diffusion-driven weak separation and flocculation of the UGCC particles, as shown in Fig. 2(a). No pigment sediment was observed, so that it can be concluded that the water layer is due to liquid phase exclusion from the floc structure of the pigment particles only and not from the fibrillar gel phase. In addition, the DGCC containing suspensions were kept standing for a longer time, up to 24 h, to evaluate their stability further. There was no evidence of water separation even after this lengthy period, as shown in Fig. 2(b), and so we may conclude that despite free diffusion within the gel held water the DGCC dispersion remains fully stable, confirming that the particles are dispersed homogeneously and remain suspended in the MNFC gel against sedimentation. Therefore, the free diffusion of pigment particles only has very limited effect on the observed dewatering process induced when applying an ultralow shear on MNFC:UGCC suspension, especially when the effect can be seen after only a relatively short period of 30 min

(see section 3.2), compared with many hours complete stability in the static state. Moreover, as an aside, there is almost no effect for a suspension of DGCC alone.

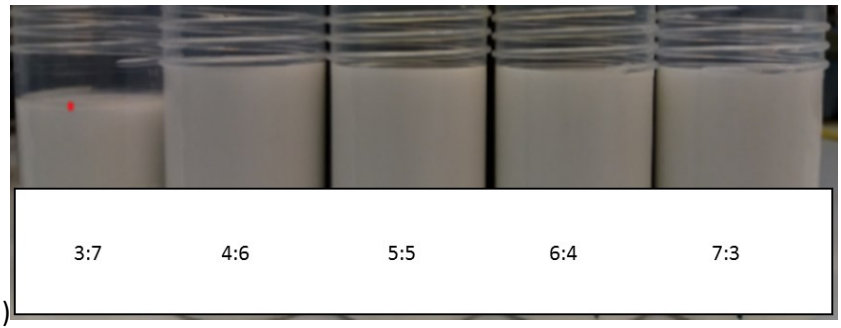

(a)

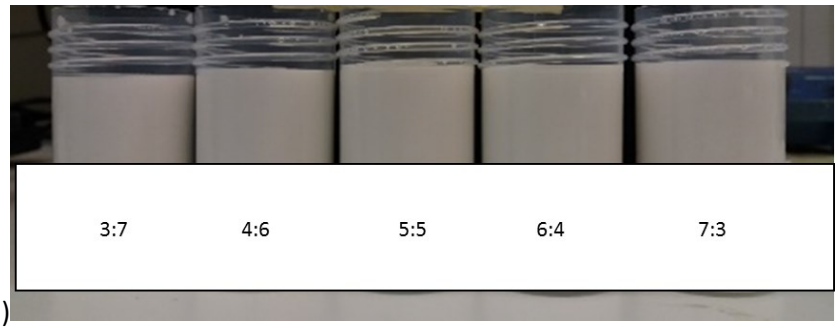

(b)

Fig. 2 (a) MNFC:UGCC suspensions after standing for 5 h - only the MNFC: UGCC, 3:7, showed a small amount of water separation (indicated by the red spot) due to free diffusion -, (b) MNFC:DGCC suspensions remain fully stable for 24 h.

3.2 Dynamic viscosity when using an ultralow shearing rate and structural/dewatering observation

The test of dynamic viscosity as a function of time for MNFC and MNFC:UGCC/DGCC composite suspensions is carried out under the uniform physical condition as described in section 2.5, as shown in Fig. 3 and Fig. 4.

Figs. 3(a) and 4(a) present the dynamic viscosity at the medium shear rate of 200 s^{-1} over 5 min for the MNFC: UGCC and MNFC: DGCC suspensions, respectively. We see that whatever the material or blend (MNFC, UGCC, DGCC, MNFC:UGCC or MNFC:DGCC) at all measured composite levels, under medium shear rate (200 s^{-1}), the dynamic viscosity remains at a respective constant level, which means that the particles of GCC remain free to flow unhindered, and this applies also to the flow within the MNFC gel-related water. This once again confirms the findings made by Dimic-Misic *et al*. 2017 [9].

Under conditions of ultralow shear rate of 0.01 s^{-1}, acting below the structure yield stress of the gel when there is sufficient MNFC present in the mix with the undispersed GCC (UGCC), Fig. 3(b), the dynamic viscosity shows the initial breakdown of the static structure (the first maximum in the dynamic viscosity curve) followed by a shear thinning and eventual structuration in the form of rheopexy, which confirms also the findings of Dimic-Misic *et al*. 2017 [9]. However, when the MNFC concentration in the mix is reduced to the lowest level, the structuration effect becomes less marked in respect to the viscosity response, though nonetheless it can be seen to be present. This confirms also that the MNFC is an essential component of the resulting structuration. In Fig 4(b) we see the contrary, in that in mixes with the dispersed GCC (DGCC) structuration is largely absent. Therefore, we can positively confirm that the structuration expressed by the

viscosity in Fig. 4(b) combines the action of the MNFC and the undispersed UGCC together. Clearly, the greater the amount of MNFC, provided undispersed pigment is also present in the MNFC:UGCC mix samples, the greater is the degree of structuring.

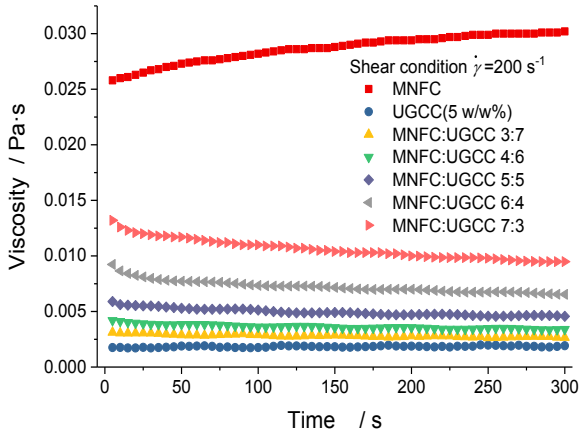

(a)

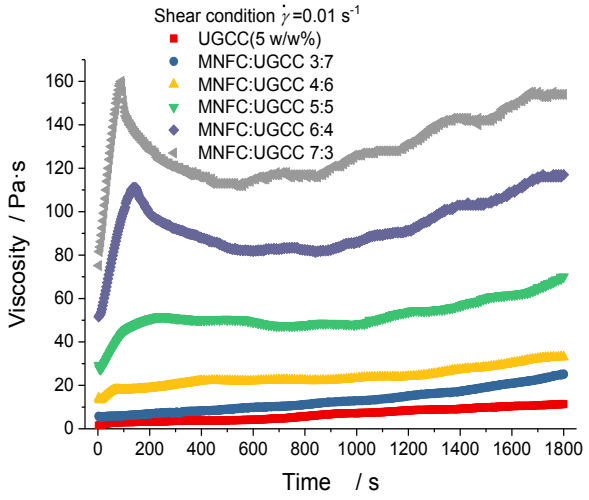

(b)

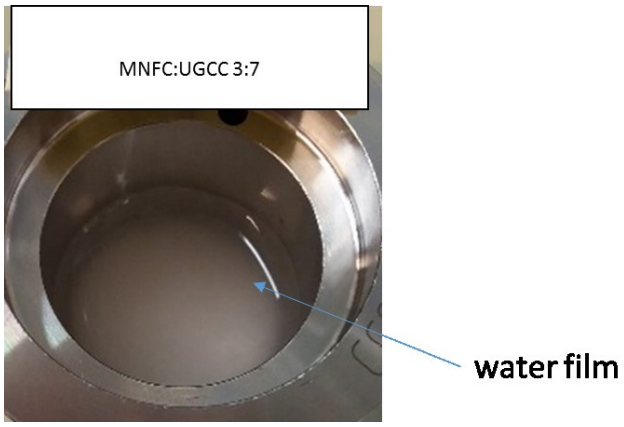

(c)

Fig. 3 MNFC:UGCC composite suspensions at shearing rates of (a) 200 s^{-1} and (b) 0.01 s^{-1}, (c) the water film on the surface clearly shows transparent, and indicates the dewatering behaviour under ultralow shear conditions as previously seen by Dimic-Misic *et al*. 2017 [9].

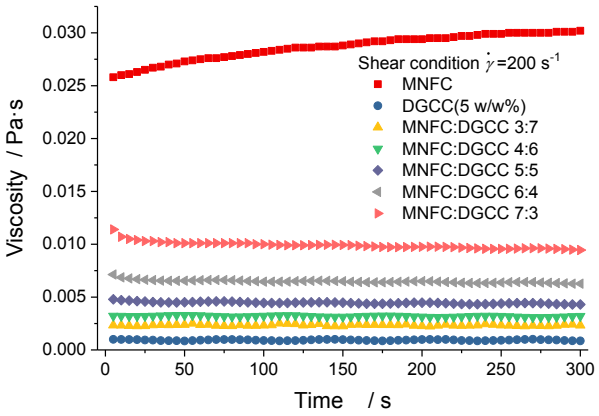

(a)

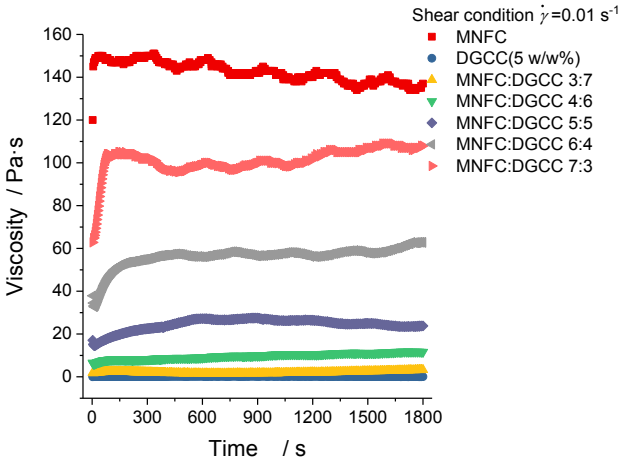

(b)

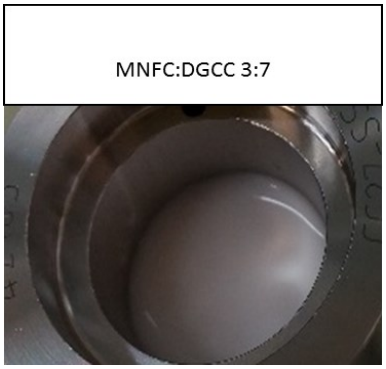

(c)

Fig. 4 MNFC:DGCC composite suspensions at shearing rate of (a) 200 s^{-1} and (b) 0.01 s^{-1}, (c) in this case of the dispersed DGCC there is no observable water film on the surface but a light reflection only from the milky-white suspension.

In Fig. 3(c) we see an illustration of the appearance of a transparent water layer on the top of the ultralow sheared sample, exemplified in the case of the MNFC:UGCC 3:7 composite suspension. The increasing values of viscosity under ultralow shear following the breaking of the gel illustrate the progressive nature of the structure-building mechanism. As the amount of UGCC is more than that of MNFC in the composite samples of 3:7, 4:6 and 5:5, the moving UGCC particles readily encounter each other and the MNFC fibrils. The unbound water is thus more easily released, Fig. 3(c). However, where the number of UGCC particles is limited, such as in samples MNFC:UGCC 6:4 and 7:3, the statistical chance of structure-building encounters is reduced and the dewatering requires significantly longer forming. Ultimately, the amount of recoverable water becomes less and less as the ratio of the UGCC component decreases. This dewatering effect on the cellulosic fibril suspension (MNFC) driven by the presence of undispersed calcium carbonate particles (UGCC) can now be contrasted with the inhibited dewatering of the comparative MNFC:DGCC 3:7 suspension containing dispersed GCC shown in Fig. 4(c), where the stabilised DGCC remains effectively inert.

Where the MNFC:UGCC samples have formed a separated water layer on the top of the suspension, a rough estimate of the water layer thickness in the rheometer cup was obtained by inserting a matt microscope slide vertically to probe the height of water coming out measured with a rule, as listed in Table 3. The amount of dewatering from suspensions is in good agreement with the dynamic viscosity changes and rheopectic

structure, as seen in Table 3, where the amount of dewatering is correspondingly reduced as the UGCC component particles are reduced in the MNFC host suspension. These findings confirm the first time observations made by Dimic-Misic *et al*. 2017 [9], where, instead of GCC, the pigment comprised PCC also in an undispersed and dispersed state.

Table 3. The amount of dewatering from suspensions after ultralow shearing expressed as % fraction of water layer thickness observed above the total sample depth, i.e. volume ratio (vol%)

Sample **Water layer** / vol%	3:7	4:6	5:5	6:4	7:3
MNFC:UGCC	24 %	12 %	8 %	4 %	< 2 %
MNFC:DGCC	0	0	0	0	0

3.2.1 Interaction during diffusion after ultralow shear

Given the impact of the induced dewatering of MNFC during the application of ultralow shear in the presence of UGCC, it is interesting to see how the subsequent free diffusion of particles affects the amount of water expelled. As can be seen in Fig. 5, the diffusion under static conditions after the cessation of ultralow shear leads to further expulsion of water in the cases of the higher concentrations of UGCC in the mix (MNFC:UGCC 3:7 and 4:6).

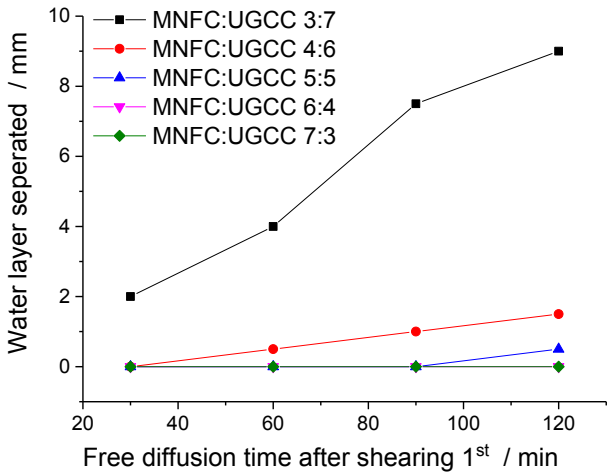

Fig. 5 Free diffusion after repeated shearing.

3.3 Optical microscopy – following the structure interactions

Here, we go on to study the physical structural changes observed by comparing optical microscope images of the samples before and after ultralow shearing. The microscope images of 3:7 and 4:6 for MNFC:UGCC/DGCC in Figs. 5 and 6 exemplify the effect of the ultralow shearing rate of 0.01 s^{-1} by comparing the state of the pigment nanoparticles in relation to the nanofibrils – the latter can be seen emanating from the microfibril backbone structure – before and after the application of ultralow shear.

In the microscopic observations, the correspondence between the physical structure and the rheology results strongly testify that the dewatering phenomenon and structuration are indeed linked. The images of

MNFC:UGCC samples 3:7 and 4:7 exemplify the process (Fig. 6). We see that the undispersed calcium carbonate particles (UGCC) become adsorbed onto the nanofibrils of the MNFC, and depending on how many carbonate particles are present, either the MNFC has insufficient adsorption capacity to remove all the carbonate particles from the liquid phase (Region A), MNFC:UGCC 3:7 in Fig. 6(c) – the detailed Region C in Fig. 6(b) –, or nearly all of the particles become adsorbed if their number is less than the adsorption saturation on the MNFC, MNFC:UGCC 4:6 in Fig. 6(f) – the detailed Region D in Fig. 6(e). It is clear to see how the nanocarbonate particles become distributed along the nanofibrils like pearls on a necklace.

The role of ultralow shearing is obviously different from medium to high shear in that the action of invisibly slow shearing leads uniquely to the adsorption of the colloidally unstable UGCC particles, which otherwise remain free either to diffuse in the gel trapped water under static conditions or to move throughout the liquid phase under higher shear. We can speculate that the dewatering effect of this adsorption arises by the further flocculation caused by the carbonate particles bridging the structures as shown by the arrows in Region B, Fig. 6(b) and (e). The importance of ultralow shear is that it brings the carbonate particle into contact with the nanofibril surface under shear strain in regions where the gel is not fully broken. Clearly free diffusion of the particles does not result in sufficient dwell time in contact with the nanofibrils for adsorption to occur. The fact that this postulated dwell time is important for adsorption leads us to propose a chemical interaction as the mechanism lying behind the adsorption effect, which phenomenon we go further to investigate in more detail in the later sections of this paper.

299

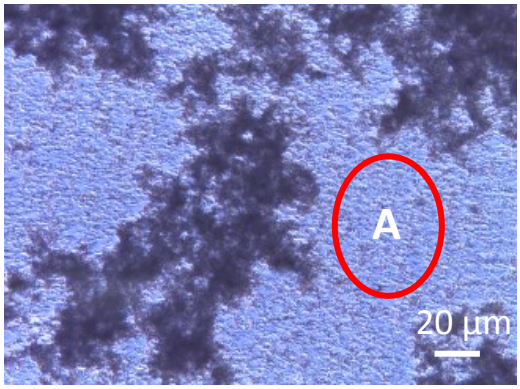

(a) MNFC:UGCC 3:7 rest state (unsheared)

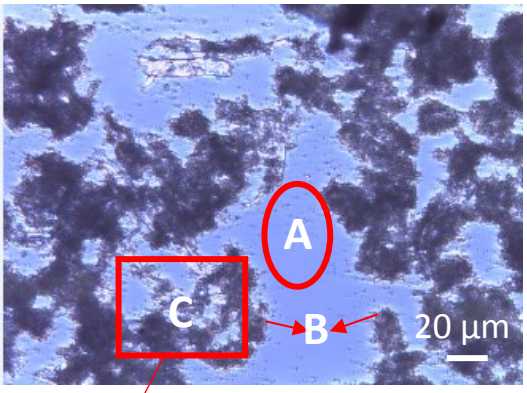

(b) MNFC:UGCC 3:7 ultralow sheared

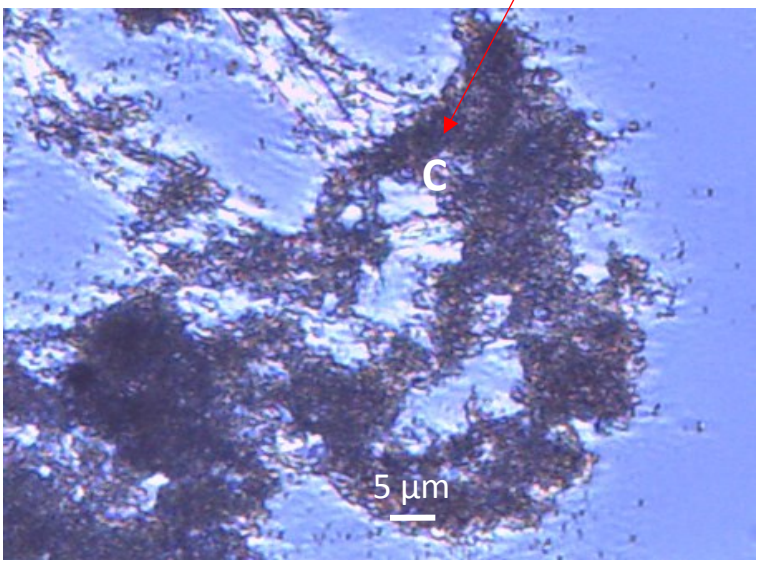

(c) detail of MNFC:UGCC 3:7 ultralow sheared

300

301

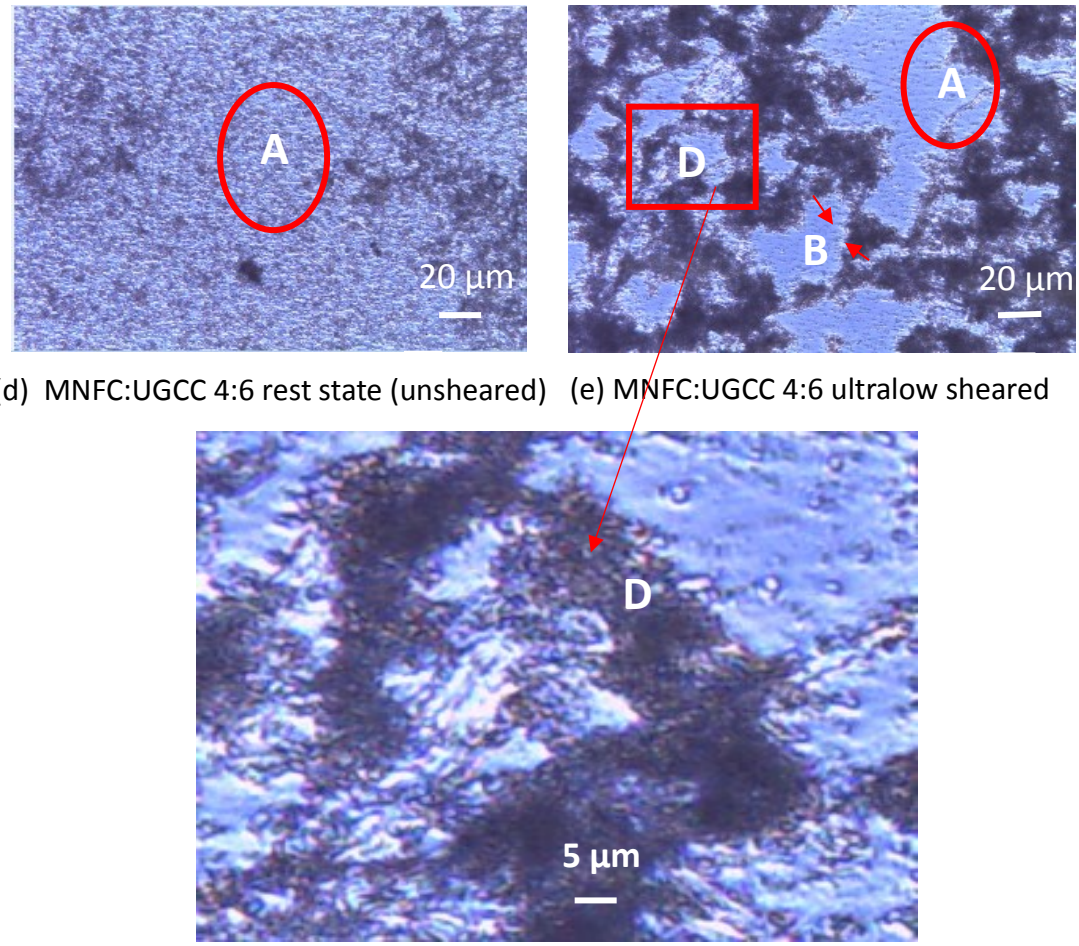

(d) MNFC:UGCC 4:6 rest state (unsheared) (e) MNFC:UGCC 4:6 ultralow sheared

(f) detail of MNFC:UGCC 4:6 ultralow sheared

Fig. 6 MNFC:UGCC 3:7 and 4:6 composite suspensions (a) and (d) in the static state after medium shearing (200 s^{-1}) and resting (unsheared), and (b) and (e) after extended time of ultralow shear (0.01 s^{-1}). The structuration is shown in more detail in (c) and (f).

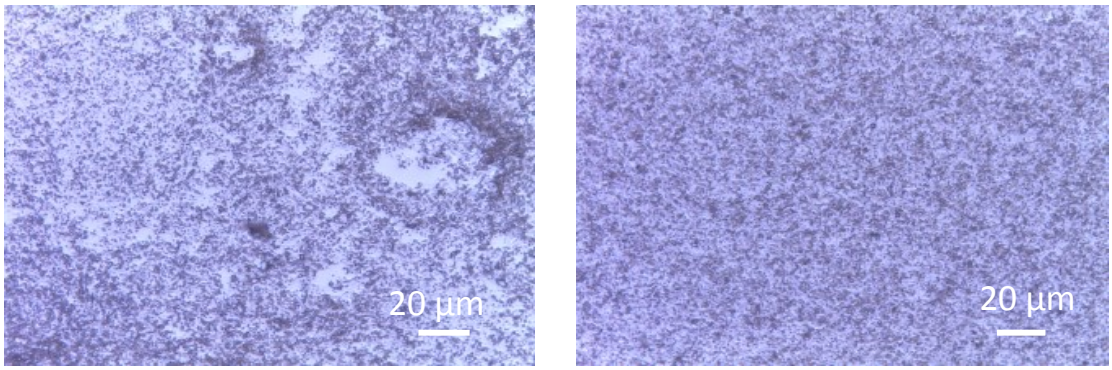

(a) MNFC:DGCC 3:7 rest state (unsheared) (b) MNFC:DGCC 3:7 ultralow sheared

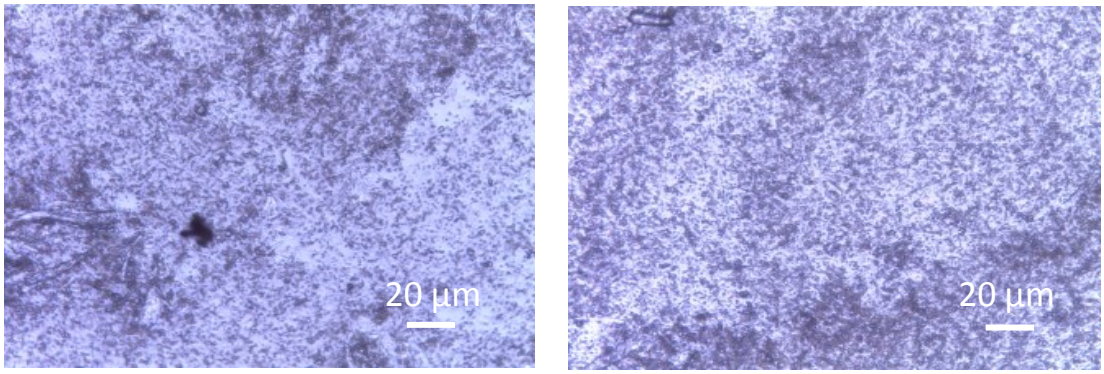

(c) MNFC:DGCC 4:6 rest state (unsheared) (d) MNFC:DGCC 4:6 ultralow sheared

Fig. 7 MNFC:DGCC composite suspensions in the (a), (c) static (unsheared) and (b), (d) ultralow sheared state, respectively. Both MNFC:DGCC 3:7 and 4:6 remain fully dispersed without structuration.

The action of polyacrylate dispersant maintains the colloidal stability of the dispersed DGCC, and so prevents any adsorption onto the nanofibrils, Fig. 7. This is supported by the high anionic charge repulsion between the two species. However, colloidal stability alone might not be the whole reason why the carbonate particles with polyacrylate on their surface fail to adsorb, but rather the chelating action of the polyacrylate might act to delay the sorption. This hypothesis will also be challenged as we move on.

It can be concluded, therefore, the rate of shear is critical in that it should enhance material contact by overcoming potential energy stability barriers, but should not be so strong as to prevent the collective structure from building. As a result, the free unbound water is progressively expelled. The schematic shown in Fig. 8 illustrates this hypothesis via the mechanistic five steps (a)-(e) leading to structuration and the observed dewatering process thus:

a) the GCC particles are suspended in the MNFC gel water in static state and are free to diffuse, however the diffusion and Brownian motion provide insufficient force and dwell time to bring the particles into intimate contact with the surface of the fibrils,
b) applying medium to high shear to this system results in the breakage of the gel and the particles moving freely in the released gel water. This acts simply to mix the system homogeneously, after which a return to the static rest state gel simply results in the situation described in a) above.
c) Application of ultralow shear results in an applied strain to the unbroken regions of the gel, which acts to force the particles into intimate contact with the nanofibril surface, maintain an extended dwell time, a factor which seems to be the key to the adsorption mechanism, such that
d) the nanocarbonate particles “decorate” the nanofibrils by adsorption along their length, and the system eventually becomes de-mixed.
e) Further shear stress then brings the adsorbed particles on the nanobrils into further contact with each other and auto-flocculation between adsorbed carbonate starts to occur, which together with continued ultralow shear then results in entanglement to form a structuration of macroscopic dimensions, seen as a continuous rheopexy, during which phase separation, i.e. water release, occurs.

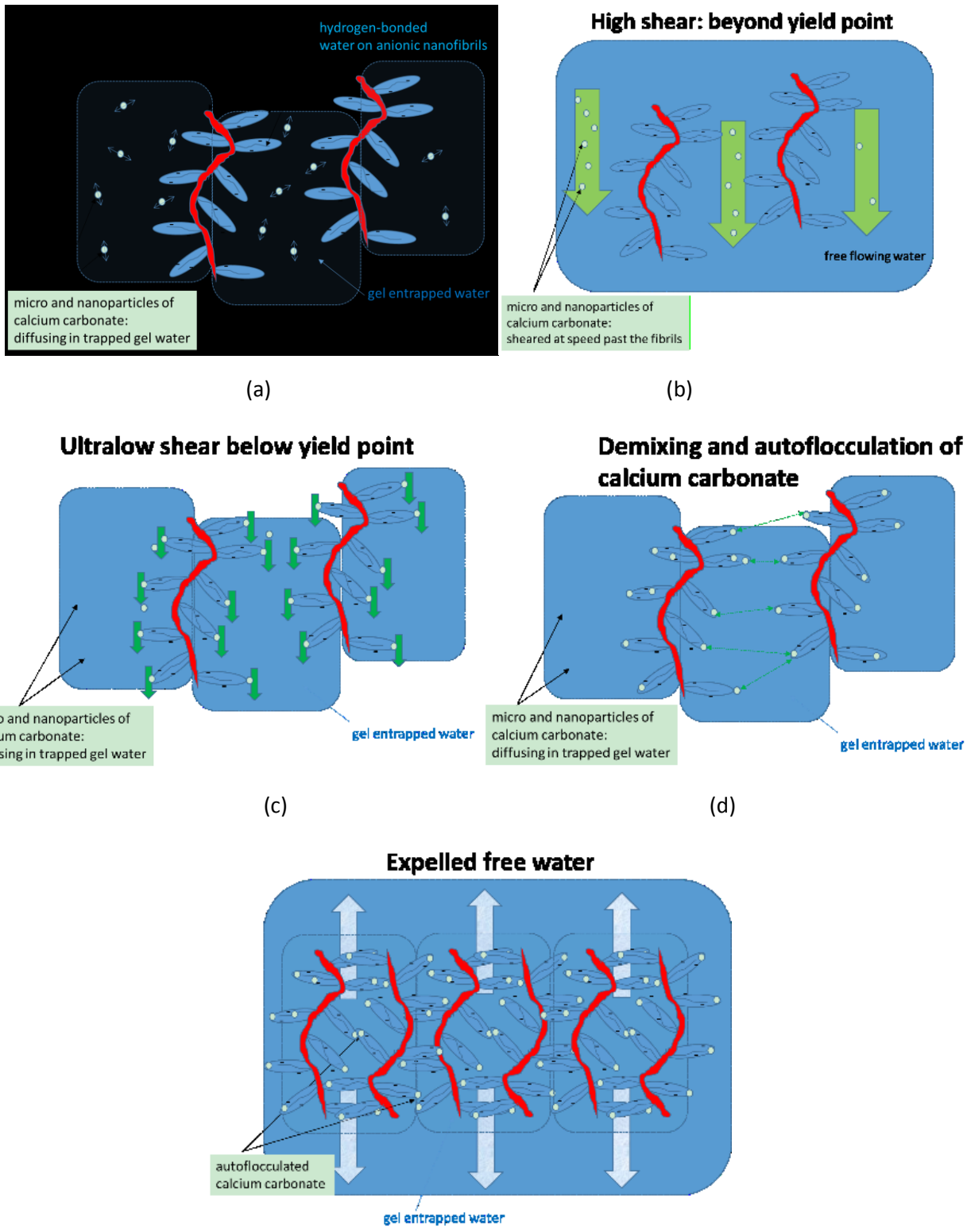

Fig. 8 The de-mixing and dewatering mechanism of MNFC:UGCC systems.

3.4 Repeated ultralow shearing for MNFC:UGCC/DGCC composite suspensions, and effect of storage

To establish the sensitivity to repeated exposure to ultralow shear we investigated the effects of short time cycling of shear application together with long time storage between cycles. Having completed the

investigation of the effect of applying a single period of ultralow shear, the samples were stored in a refrigerator for 5 days, and then sheared again under the previous protocol of ultralow shearing rate. Finally, they were sheared for a third time a further day later. Prior to ultralow shear application, the samples were re-mixed with a magnet bar stirrer for about 30 min to redistribute any weak flocculation and to provide a homogeneous suspension.

In this discussion it is important to stress that the single components used throughout the experiments were stored similarly under refrigerated conditions. Thus, where freshly made mixes behave differently from stored mixes we may conclude that the effects arising as a function of time are related purely to interactions occurring in the mix and not related to component aging or bacterial degradation.

3.4.1 Repeated dynamic viscosity response of MNFC:UGCC suspensions

The viscosity response to repeated ultralow shear application with storage between is shown in Fig. 9. After several days storage, the dynamic viscosity of MNFC:UGCC suspension under ultralow shear increased much more strongly as a function of time than before. Moreover, it can be seen that multiple application of ultralow shear reveals that the initial driving mechanism for structure build is largely retained, and that the viscosity level is raised as the structuration is effectively continued once the gel-hardening structure in each case is broken. It could be concluded further, therefore, that the structuration responsible for dewatering is an irreversible adsorption of the UGCC on the initial surface layer of nanofibrils under these ultralow shear conditions, and distinctly separate from the viscoelastic gel structure formed at rest, as was previously deduced from the rheopectic behaviour which we see repeated at a higher level in the second and third applications of shear.

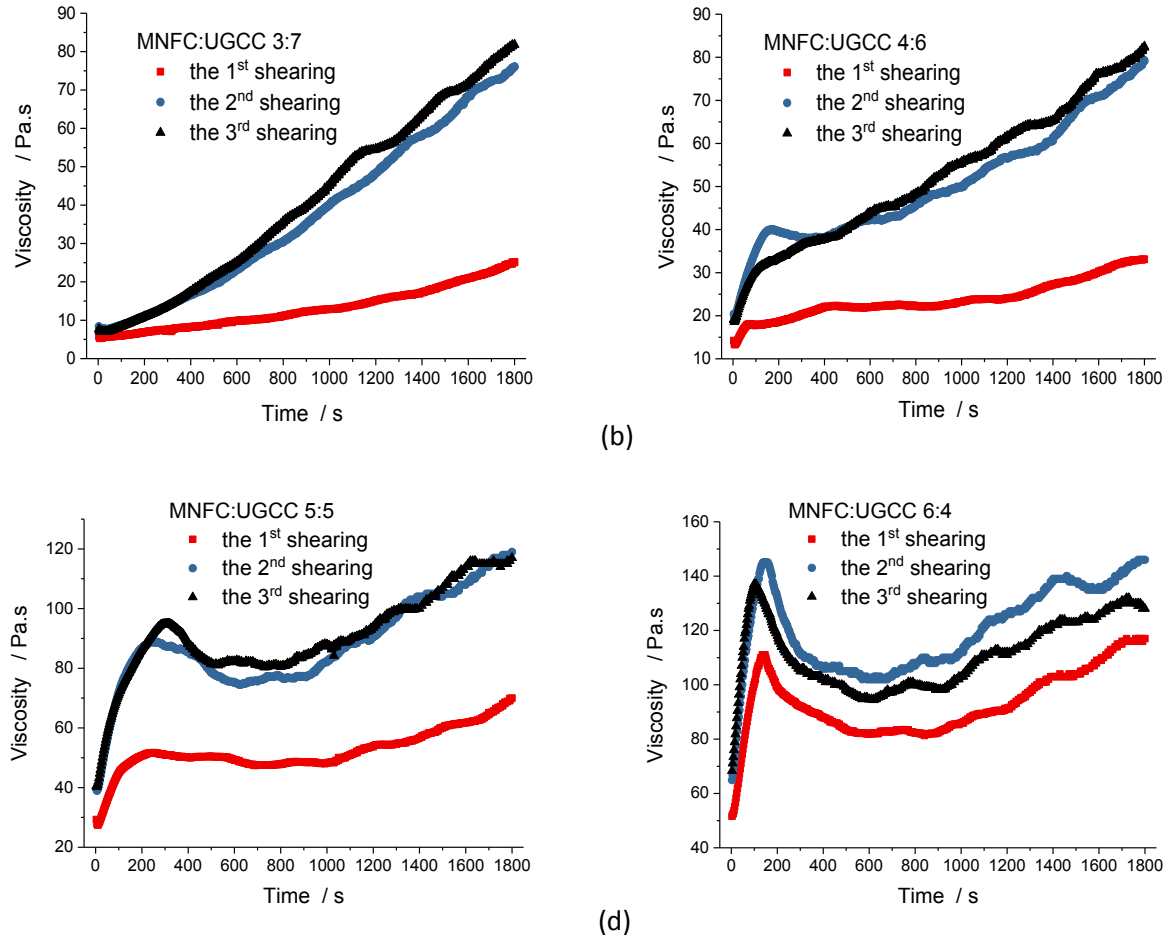

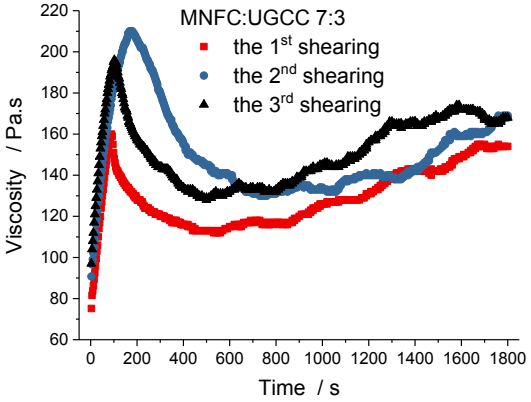

(e)

Fig. 9 Repeated application of ultralow shear after lengthy periods between for MNFC:UGCC (a)-(e): 1st shearing is prior to storage, as shown in Fig. 3(b), the 2nd and 3rd shearing are each after sequential storage periods.

The amount of water separated is also directly correlated with the changes of dynamic viscosity, being greatly increased compared with during the initial shearing, as seen in Fig. 10. It can be seen that the multiple application of ultralow shear leads to a significant increase in dewatering levels for those samples with the higher levels of UGCC, e.g. 3:7 and 4:6 showing approximately a factor of 2 greater dewatering. The efficiency of dewatering is thus much increased while the structure building mechanism responsible for dewatering remains stable over time.

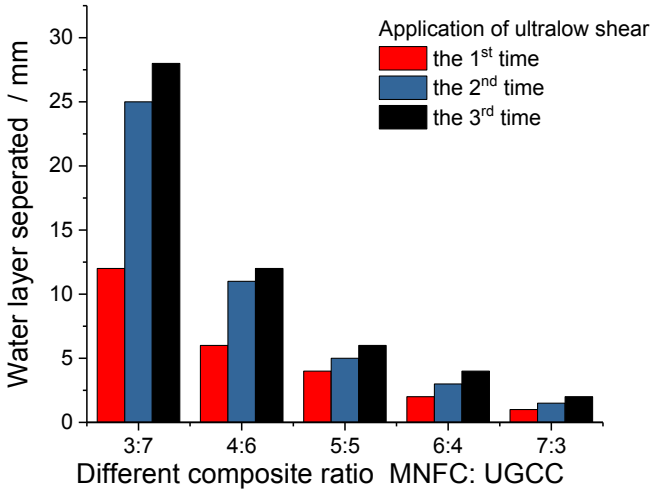

Fig. 10 Dewatering layer thickness from a constant total depth of sample as a function of repeated applications of ultralow shear each following a period of storage for MNFC:UGCC.

3.4.2 Repeated dynamic rheological response of MNFC:DGCC suspensions

The dynamic rheological responses to repeated ultralow shear application when substituting the undispersed with the dispersed GCC are shown in Fig. 11. After 5 days storage after the first shear with an ultralow shearing rate, a huge difference is seen in the dynamic viscosity response for the MNFC:DGCC sample ratios 3:7, 4:6 and 5:5, i.e. in those cases where the mass fraction of DGCC particles is more than or equal to the fraction of MNFC in the composite mix. When the amount of DGCC particles in the sample is less, then the

change in viscosity due to storage and re-shearing at ultralow shear rate reduces strongly. Once again, therefore, we can assume that the interaction between the components is the key factor in the storage effect.

As in the case of the undispersed GCC particles in the MNFC:UGCC mixes, the observed dewatering increase for MNFC:DGCC also follows the increasing dynamic viscosity response as shown in Fig. 12. The separated water layer, however, is not clear water but appears milky, as seen in Fig. 11(f). This suggests that, unlike the UGCC particles, the DGCC particles have not been as efficiently adsorbed onto the nanofibrils over time but some still remain stable in suspension after de-mixing from the gel. However, clearly some do structure-form with the nanofibrils since the more DGCC is in the sample mix, the greater is the water layer separated, but it is clearly not as much as in the undispersed particle case, and contains the remaining amount of non-adsorbed dispersed GCC particles. In addition, interestingly, if the samples are vigorously re-mixed and left to stand for 24 h under conditions of free diffusion after the 2nd and 3rd ultralow shear application, the dewatering also increases, Fig. 13, whereas previously there was no dewatering effect on standing after the first ultralow shear application in this dispersed DGCC containing case.

In respect to the re-dewatering effect caused by repeated ultralow shearing and storage, it is clear that a significant portion of the DGCC particles become colloidally destabilised and begin to flocculate, and during the ultralow shear progressively become adsorbed on the nanofibrils, creating structuration by aggregation while the remaining still stable particles are found in the separated gel water phase. The end effect is that the DGCC evolves into a mix of DGCC and effectively UGCC over time in the presence of the MNFC under conditions of storage and repeated ultralow shear application, and thus the derived destabilised particles behave according to the mechanistic proposal summarised schematically in Fig. 8.

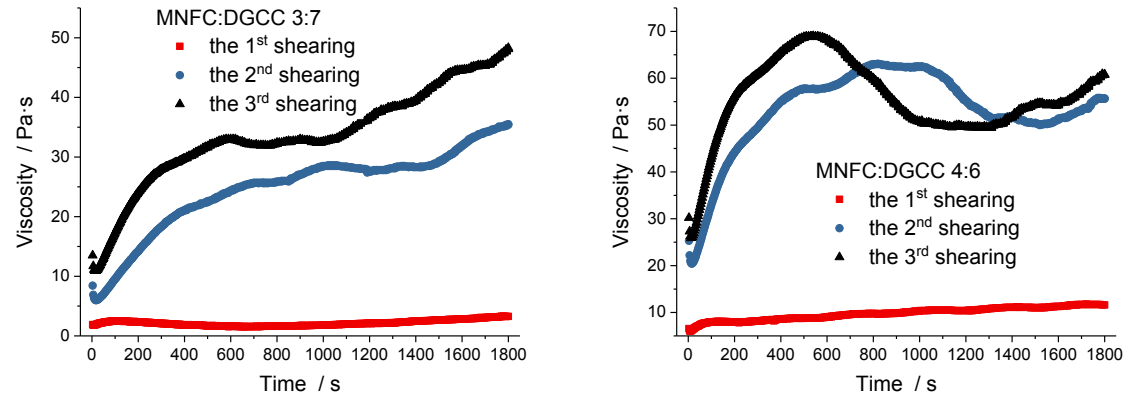

(a) (b)

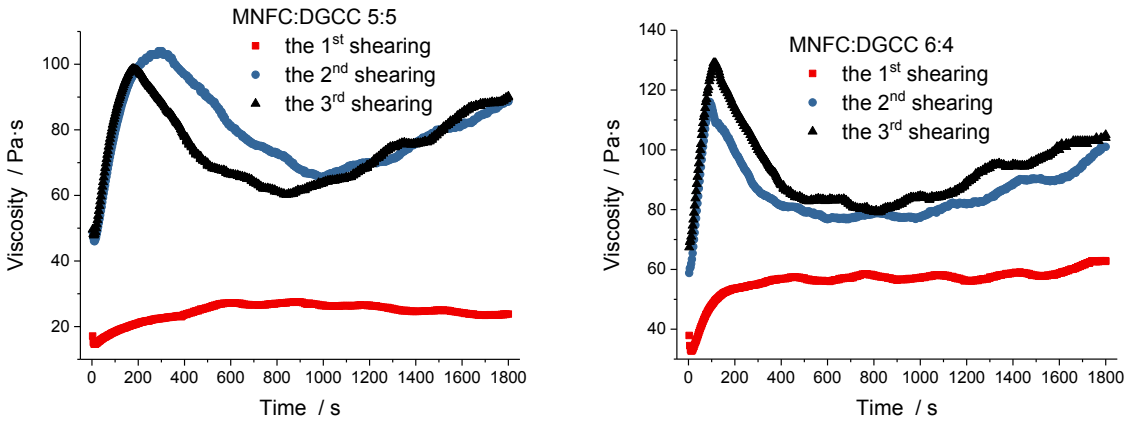

412 (c) (d)

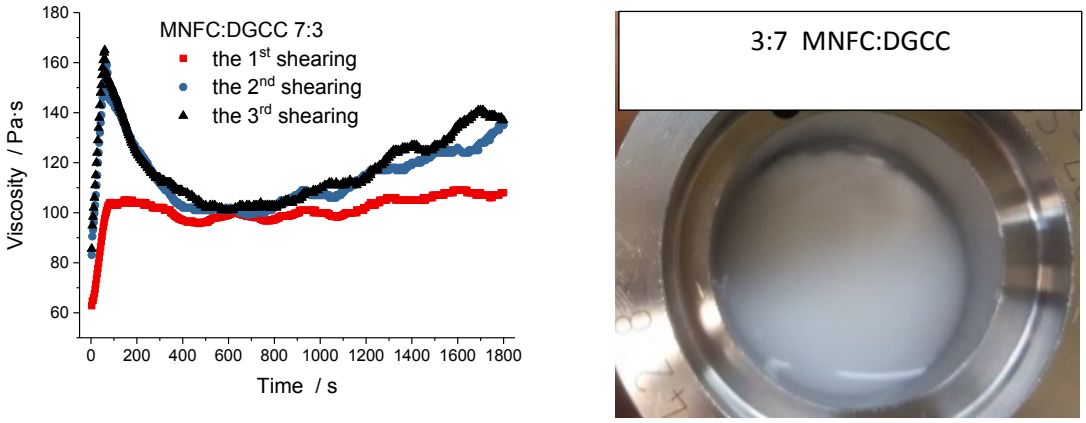

413

414 (e) (f)

415 **Fig. 11** Repeated application of ultralow shear, each after lengthy periods of storage, for MNFC:DGCC (a)-(e).
416 The dewatered turbid (milky) layer can be seen in (f).

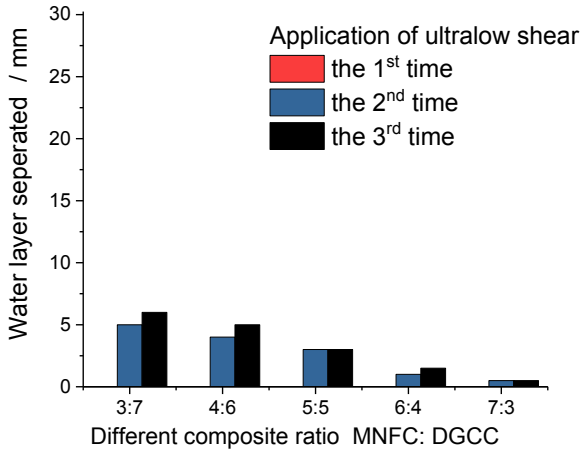

417

418 **Fig. 12** Dewatering layer thickness formed on samples of constant depth as a function of repeated
419 applications of ultralow shear each following a period of storage for MNFC:DGCC.

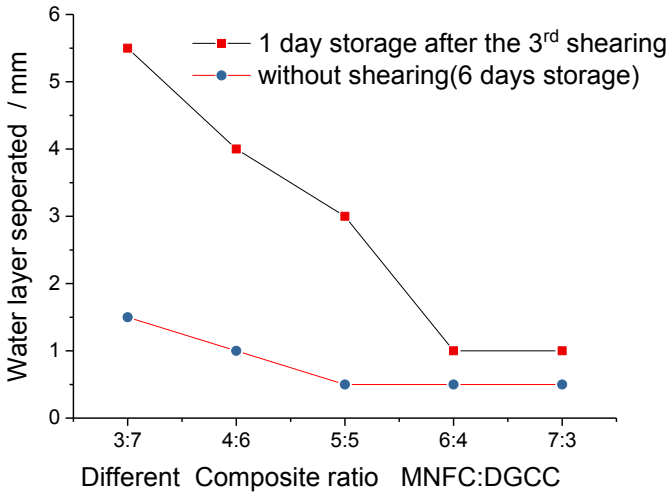

Fig. 13 Adsorption by free diffusion enhanced after storage for MNFC:DGCC, illustrating the progressive destabilisation of dispersed calcium carbonate and the impact of the application of ultralow shear.

3.4.3 Investigating the reason for DGCC destabilisation in MNFC:DGCC samples due to repeated shearing with storage

At this point, we investigate the mechanism behind the slow interaction between dispersed calcium carbonate particles and the nanofibril surface, manifest by the progressive dewatering tendency in response to ultralow shear rate after long term storage, as this will reveal the role played by the surface chemistry on the nanofibril surface, i.e. the action of the adsorbed water layer on the fibril surface on the particles and chelating agent (polyacrylate) adsorbed on the calcium carbonate.

To explore and explain the reason for the dewatering effect for MNFC:DGCC arising during recycling shear with storage time, freshly prepared samples were sheared at ultralow shear rate five times, with respective intervals of storage prior to each shear experiment of 1 day before the 1st application (1st), 5 days between the second and third (2nd-3rd), 10 days between the third and fourth (3rd-4th), and 20 days between the fourth and the fifth (4th-5th). The average pH_{Av} and conductivity of each sample were recorded before and after each shearing, and a reference without shear applied was included, Fig. 14(a)-(e). The pH of the original MNFC (5 w/w%) without any added calcium carbonate particles is ~5.73. We see that the pH of all sample mixes reduces continuously as a result of the ultralow shear (0.01 s^{-1}) and with interval time. In parallel, the conductivity is seen to increase, which means that as the dispersed DGCC gradually becomes destabilised and, under shear, adsorbed onto the nanofibril surface the ionic strength increases. The likely action for this is proton exchange for calcium ion. Given the Ca^{2+} ion generation, we are led to suspect that the surface of the MNFC nanofibrils is revealing a potential for proton release during the process of shearing and storage.

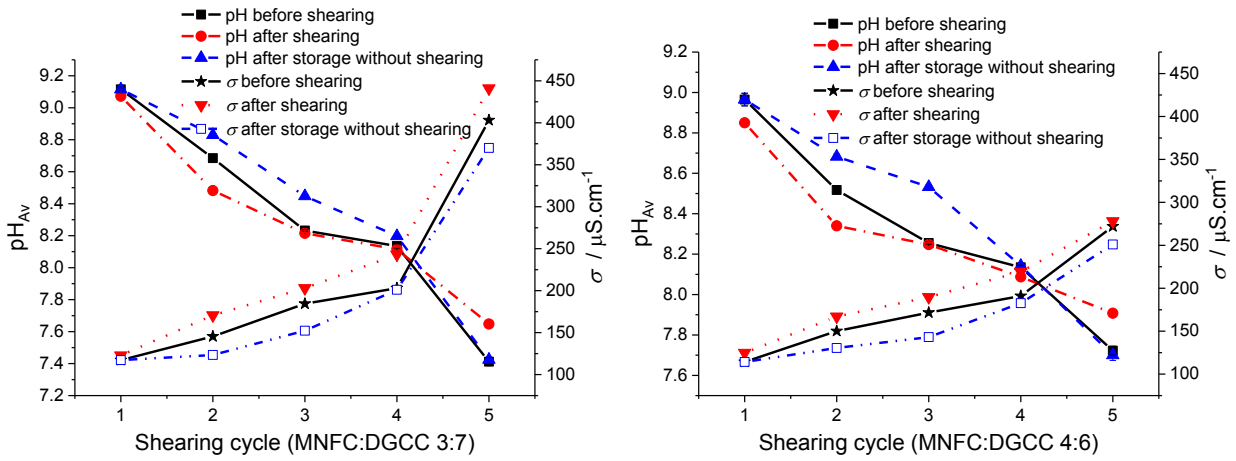

443

444 (a) (b)

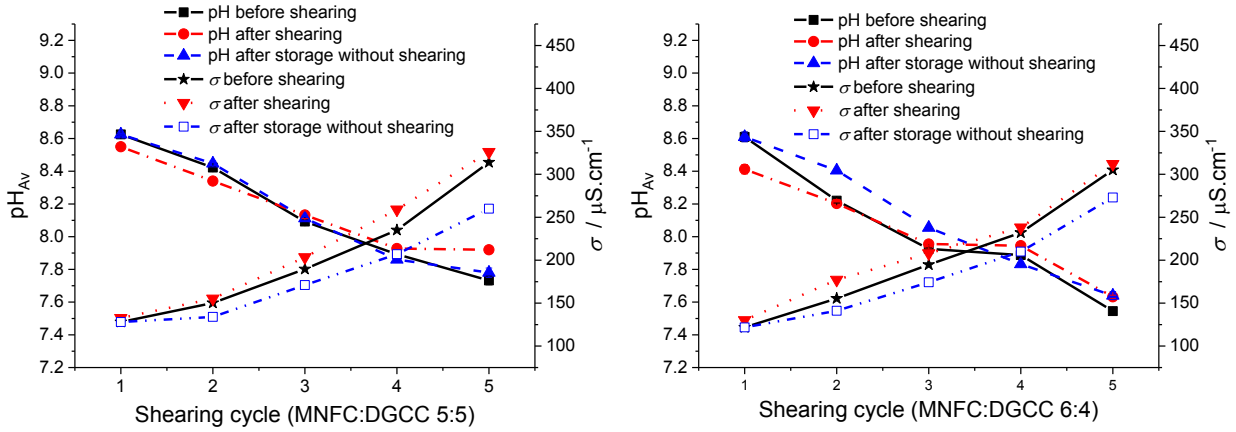

445

446 (c) (d)

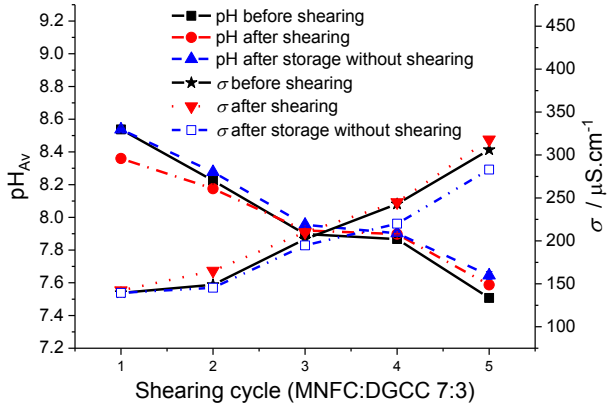

447

448 (e)

449 **Fig. 14** The average pH_{Av} drop and conductivity increase over time at the given shear intervals for MNFC:DGCC
450 samples.

451 Addition of calcium carbonate to the original MNFC suspension raises the pH from 5.7 to the natural pH of
452 calcium carbonate ~8.5. After the first shearing, for all samples, the pH changes are quite small, from -0.04

for sample of 3:7 to -0.2 for sample of 7:3, Fig. 14. That the pH change is slightly greater with lower amounts of calcium carbonate present suggests that the calcium carbonate is continuing to act at first as a buffer, maintaining the pH close to 8.5. The conductivity also remains almost constant before and after the first shearing for all the samples, suggesting that the calcium carbonate is not at this stage releasing calcium ions. We, therefore, can conclude that at the first application of ultralow shear, the dispersed DGCC particles are brought close to the nanofibrils of MNFC but nearly all remain stable and free in suspension. We thus, cannot see any water separated from the sample during the first period of ultralow shear. This correlates with the earlier finding that the rheological behaviour remains almost a constant, as seen in Fig. 11.

During the process of storage after the first shearing, the dispersed DGCC particles begin eventually to experience reduced pH conditions in the bulk suspension. As a result they react with the weak acid environment. That the carbonate no longer acts as buffer, despite its continued plentiful presence, we can understand in the light of the action of the weak acid and chelating agent present and/or conjugate base formation described by Passaretti [15]. An equilibrium is established between the calcium carbonate and weak acid in relation to Ca^{2+} capture as a chelate with the polyacrylate dispersant and/or the formation of the conjugate base. This prevents excess dissolution of the calcium carbonate under these reducing pH conditions. Thus, the conductivity increases controllably without the pH being raised by continuous calcium carbonate dissolution.

Following the application of a second cycle of ultralow shear after the storage period, we see that the pH is once again stable at the value prior to shearing, but at the lower value reached during storage. Thus, the acid tolerance mechanism is still largely active as the conductivity remains the same before and after the shear, but again at the slightly raised level reached during storage. This pattern of gradual pH drop continues during the subsequent storage and shearing cycles until, in the case of MNFC:DGCC 3:7 and 4:6 where the calcium carbonate portion is at its higher levels, Fig. 14(a) and (b), the conductivity suddenly rises dramatically and the pH falls steeply at the fifth cycle. This critical point occurs, therefore, when the Ca^{2+} chelating capacity of the poylacrylate present is saturated as the system returns strongly toward the pH of the starting MNFC suspension. At this point, the calcium carbonate is no longer stable in dispersion and the action of the ultralow shear in bringing the carbonate particles in contact with the nanofibril surface initiates adsorption of the particles to the fibrils due to the extended dwell time and proximity of contact. The result is structuration and water release as the previously dispersed calcium carbonate sample behaves now like the undispersed sample, no longer remaining stable against adsorption.

The experimental phenomenon observed and discussions above allow us to formulate the following hypothesis for subsequent testing.

i. The surface of MNFC nanofibrils, consisting of adsorbed water in a restrained state, donates H_3O^+ progressively to the interface with the free aqueous phase, resulting in a progressive drop in pH despite the initial buffering action of calcium carbonate associated with the formation of HCO^- and CO_2.
ii. Undispersed calcium carbonate becomes immediately susceptible to this interface acidic moiety once it is brought into intimate contact with the nanofibril surface under the action of ultralow shear, and as a result the particles of calcium carbonate become adsorbed onto the nanofibrils via Ca^{2+} bridging and thereby the formation of an insoluble salt.
iii. Dispersed calcium carbonate, with polyacrylate on the particle surface, on the other hand exhibits a degree of acid tolerance to weak acid, such that the application of ultralow shear initially fails to promote adsorption.
iv. Extended time in suspension in the presence of MNFC results in eventual saturation of the chelating capacity of the polyacrylate dispersant for Ca^{2+} ion, such that at a critical point the pH drops steeply

and the conductivity rises rapidly, resulting in a situation similar to that for undispersed calcium carbonate for at least some of the carbonate particles, and so we return partly to condition ii. above.

v. The result of carbonate particle adsorption is structuration under ultralow shear, via auto-flocculation of the adsorbed carbonate, and the associated dewatering. In the case of undispersed calcium carbonate, the water expelled is clear, whereas in the case of the dispersed calcium carbonate, at the critical point of the start of chelate saturation, the expelled water contains a portion of stable particles of carbonate remaining in suspension, and so appears turbid (milky).

Once again, we see that the amount of GCC present is a major factor in that the more there is present in the mix, the higher the starting pH. As a result, therefore, in the case of the dispersed calcium carbonate, the more that is present, the longer it takes to reach the critical point of surface Ca^{2+} release and eventual nanofibril adsorption. This is best illustrated by the cross over point between pH dropping and conductivity rising in the MNFC:DGCC suspension shown in Fig. 14. In parallel, the amount of water expelled under the resulting structuration is decreased as we move from the ratio MNFC:GCC 3:7 to 7:3 because of the reduced amount of GCC particles and increased amount of MNFC in the composite samples, as was seen in Fig. 12.

An interesting observation to note in Figs 14(d) and (e) is that there is a slight plateau of pH after the critical point. This effect corresponds with the cases where there is less dispersed carbonate, MNFC:DGCC 6:4 and 7:3, and hence less dispersant polyacrylate present, which suggests that the particles as they adsorb onto the nanofibrils indeed establish a conjugate base on the nanofibril surface and so act as a neutralising agent prior to subsequent further pH decrease over time, which also supports the hypothesis that the nanofibril surface can be expected to have a weak pK_a in respect to the dissociation constant K_a for the formation of H_3O^+. Additionally, the conductivity is seen to increase as a function of adsorption, as driven by the action of the ultralow shear at the critical point, supporting also the concept of the formation of Ca^{2+} at the particle-nanofibril interface. Moreover, the pH fall of all the samples after the 5^{th} cycle of shearing (post the critical point) is significantly slowed compared with the previous cycle prior to it, which suggests that more and more Ca^{2+} is released into the suspension as the calcium carbonate dissolves gradually, thus increasing the resistance to pH drop. This latter effect is, naturally, most marked for the sample MNFC:DGCC 3:7, related to the greater amount of carbonate present. The separated water amount will therefore reach a maximum in this region of cyclical shearing. The proposed mechanism is captured schematically in Fig. 15.

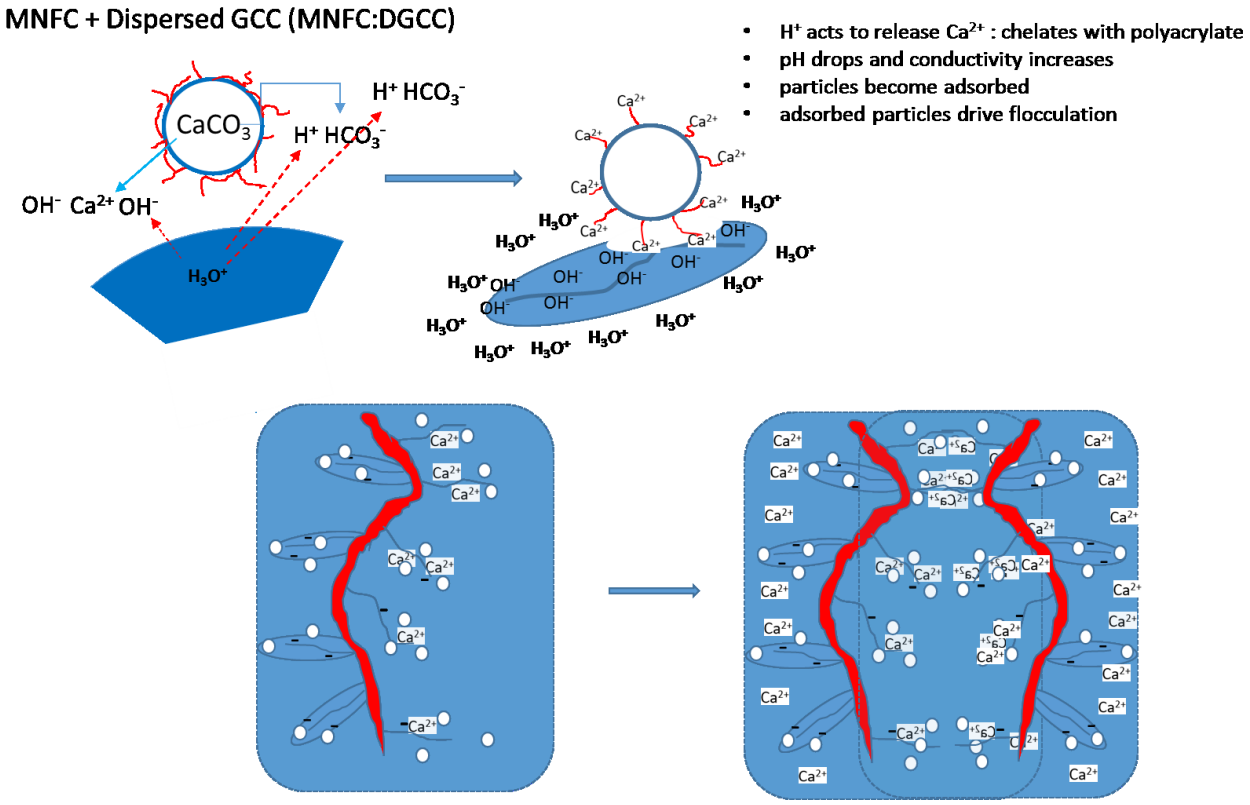

Fig. 15 Dissociated Ca^{2+} from H_3O^+ etched $CaCO_3$ particles first becomes chelated with poylacrylate and then when saturated leads to adsorption onto the nanofibrils under the action of ultralow shear.

3.4.4 Using tris buffer to stop the pH drop independently

To explore further the mechanistic hypothesis of induced dissociation of the GCC particles by a weakly acidic nanofibril surface, tris buffer was used to reduce the impact of the weak acidic action on the bulk pH of the suspension. The pH of the MNFC was set to 7.03 prior to the addition of GCC to form a further set of samples. What is seen is that the dispersed calcium carbonate when present at lower levels is unable to raise the starting pH upon addition of the MNFC to its natural level > 8. This strongly supports the proposed acid tolerant behaviour of the dispersed calcium carbonate in the presence of weak acid. The whole experimental process using ultralow shear cycling with various storage times between each cycle was repeated as described in section 3.4.3. At the first application of ultralow shear, the pH for all samples remains the same before and after shear, as does the conductivity, Fig. 16. As the storage time proceeds, the capacity of tris buffer to buffer the system becomes rapidly consumed by the weakly acidic surface of the MNFC. During the process of storage, the DGCC particles lose any further pH protection of the buffer and the Ca^{2+} dissociation occurs with the expected formation of CO_2, and hence $H^+ HCO_3^-$, driving the pH down. Meanwhile, the conductivity of the sample is seen to increase as before when no tris buffer was present. In addition, as discussed also previously, the pH drop of the samples becomes arrested somewhat eventually after long time storage due to further calcium carbonate dissolution under shearing as the GCC particles are brought into contact with the weakly acidic surface layer on the nanofibrils, Fig. 16.

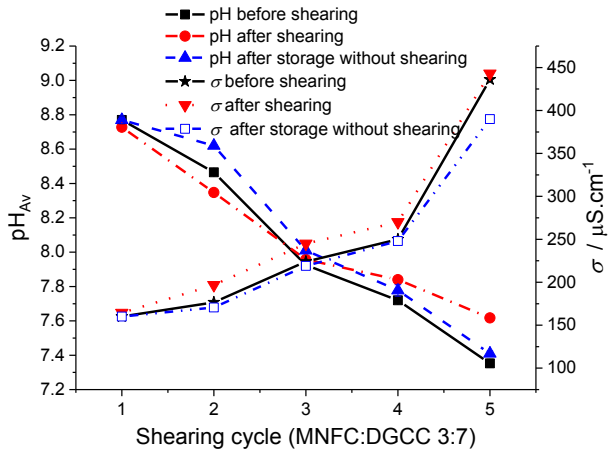

547

548 (a)

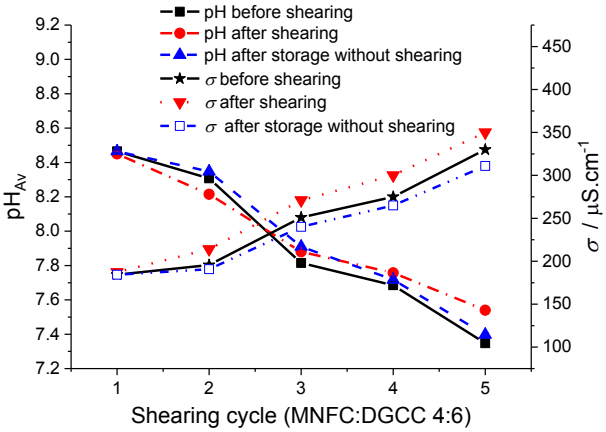

(b)

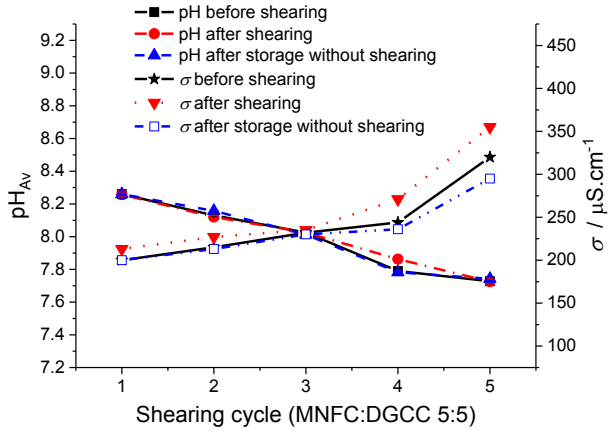

549

550 (c)

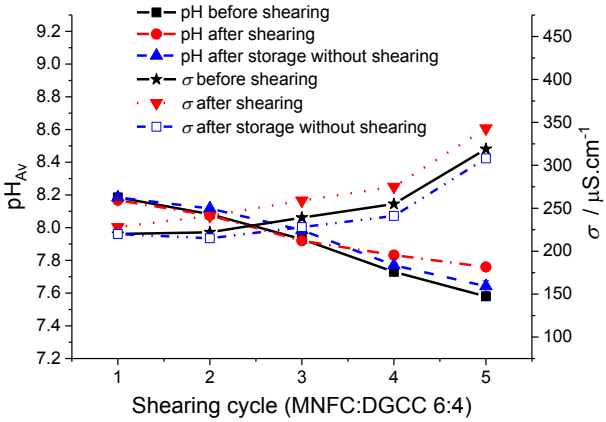

(d)

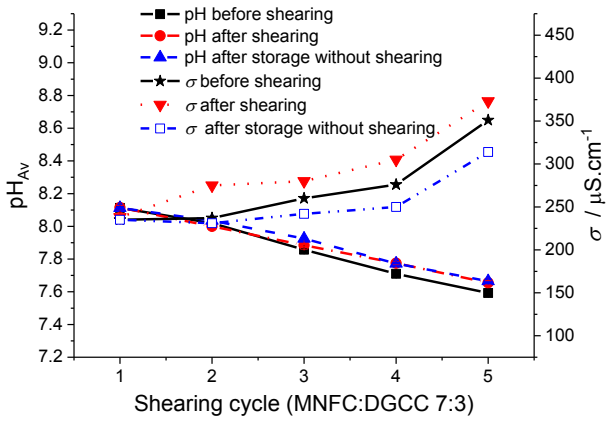

551

552 (e)

553

554 **Fig. 16** pH and conductivity changes for MNFC:DGCC samples in the presence of tris buffer (a)-(e). The buffer
555 lowers the starting pH below that of the natural level for calcium carbonate, but the mechanism proceeds as
556 seen previously without buffer once the buffer capacity is consumed.

3.4.5 The evidence for calcium ion release at the carbonate-nanofibril interface only, prior to release into solution

Reviewing the mechanistic evidence so far, the next challenge required to test the hypothesis is to confirm the order of calcium ion release, i.e. firstly at the calcium carbonate-nanofibril contact interface, and only subsequently released into the bulk aqueous phase. If the conductivity were to have risen rapidly during the first cycles of shear and storage due to rapid release of Ca^{2+} then the dispersed carbonate DGCC would rapidly flocculate as the surface secondary layer would have been compressed (DLVO theory) [16, 17]. To test this, calcium ion concentration was artificially raised by adding calcium chloride solution (0.1 w/w% concentration $CaCl_2.2H_2O$), providing dissociated Ca^{2+} and Cl^-. The MNFC:DGCC 3:7 composite sample is used here to exemplify the effect. Adding 0.5 cm^3 $CaCl_2$ solution into ~40 cm^3 suspension of MNFC:DGCC 3:7, we can see in the microscope images, Fig. 17, the indicated interaction of Ca^{2+} with the suspension mix. MNFC:DGCC without adding any added Ca^{2+} shows that the GCC particles are dispersed evenly in the suspension with a few particles already adsorbed on the surface of MNFC fibrils, as marked by the ringed areas in Fig. 17(a). The sample with added Ca^{2+} shows a clearly different structure, where some particles are adsorbed on the surface of fibrils as shown marked in black rings, and others strongly flocculated still remaining in the aqueous phase, as presented Fig. 17(b) marked by red rings, in which the part A is magnified to confirm the detail structure of flocculation, as shown in Fig. 17(c). When the addition of calcium chloride solution is increased to 1 cm^3, the number of flocculated particles obviously increases, Fig. 17(d), as confirmed at higher magnification of the marked region B, shown Fig. 17(e).

In parallel, the sample without added Ca^{2+} was also stored for 1 day (24 h) to check the status of whether Ca^{2+} is released due to the weak acid mechanism acting on the GCC particles. As we see, the dispersed GCC remains stable over this time period and is seen predominantly in the aqueous phase, Fig. 17(f), which further supports the hypothesis that the Ca^{2+}, at first is released when in contact with the surface of the fibril only and not directly in the bulk suspension due to the chelating effect of the dispersant on the DGCC particles when in the in bulk weak acid environment, as the remaining particles in the water would otherwise have become flocculated once the Ca^{2+} enters into suspension.

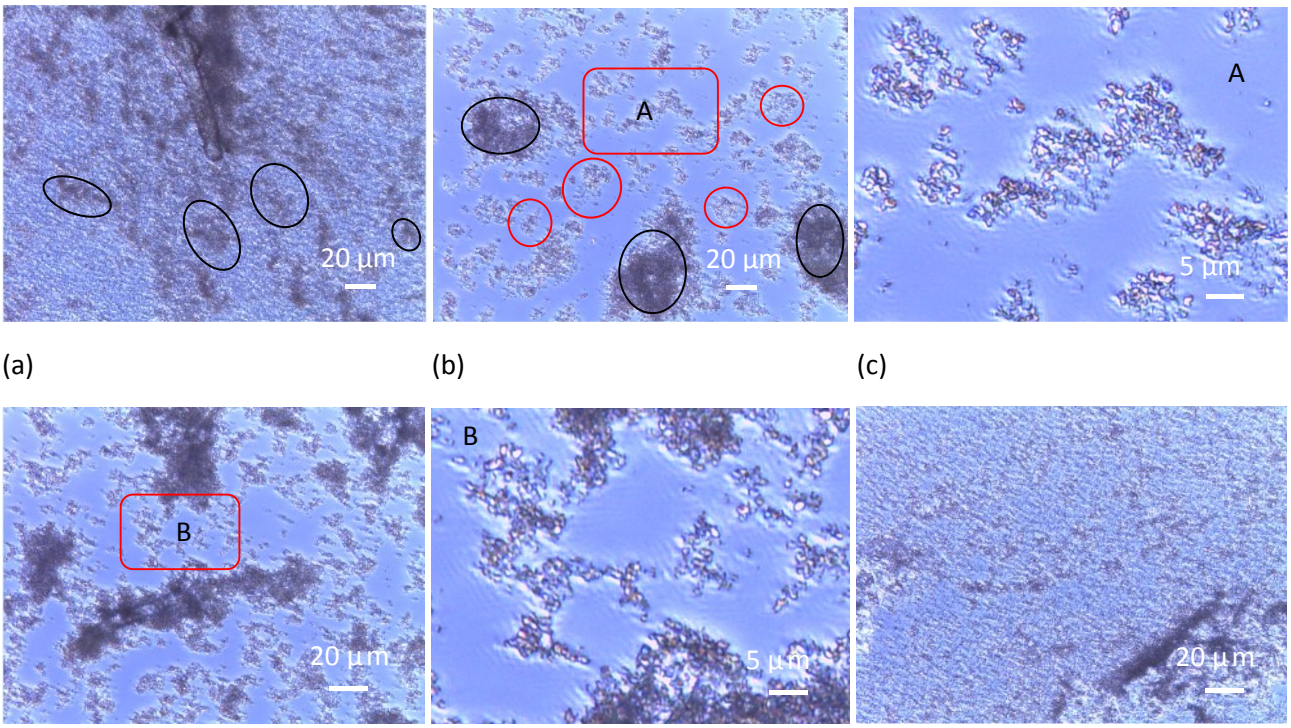

(d) (e) (f)

Fig. 17 Microscope images for the sample MNFC:DGCC with Ca^{2+} added artificially: (a) MNFC:DGCC 3:7 (no added Ca^{2+}), (b) adding 0.5 cm^3 $CaCl_2$ solution showing particle flocculation, (c) enlarged Region A, (d) adding 1 cm^3 $CaCl_2$ solution showing particle flocculation, (e) enlarged Region B, and (f) without adding Ca^{2+} but storage for 24 h

3.4.6 The evidence for the action of weak acid at the carbonate-nanofibril interface and not in the bulk

Since the pH of the composite samples of MNFC:DGCC after sequential application of ultralow shear and storage was seen to decrease from as high as around 9.1 to 7.4, due to released H^+ HCO_3^- we artificially added weak acid to mimic this process of dropped pH to verify the structural change due to Ca^{2+} activation on the carbonate surface and not release as mentioned above in the bulk phase. The acid chosen for the experiment was acetic acid, CH_3COOH. The sample MNFC:DGCC (3:7) is again used to exemplify this simulated surface activation. To ~44 cm^3 of MNFC:DGCC 3:7, as prepared in the Materials section 2, was added CH_3COOH at solution concentrations 1 w/w%, 5 w/w% and 10 w/w%, respectively using 0.5 cm^3, 0.2 cm^3 and 0.1 cm^3 doses to achieve a range of closely spaced pH, dropping, also respectively, to pH 7.60, pH 7.41 and pH 7.42. The microscope images for these samples were observed immediately, as shown in Fig. 18. In Fig. 18(a), for the sample with 1 w/w% concentration CH_3COOH, there is almost no flocculated or aggregated particles free in the suspension, but the acid addition causes both materials, calcium carbonate and cellulose to flocculate into an homogeneous mass rather than the particles of pigment adsorbing differentially onto the nanofibrils. The sample using 5 w/w% concentration CH_3COOH shows the same effect, as seen in Fig. 18(b). However, when adding the 10 w/w% concentration CH_3COOH into the suspension, there is instant pH acid shock such that some of the particles immediately autoflocculate before they can flocculate with the cellulose, and thus become size excluded and remain in the suspension in an acid-aggregated state, Fig. 18(c-d).

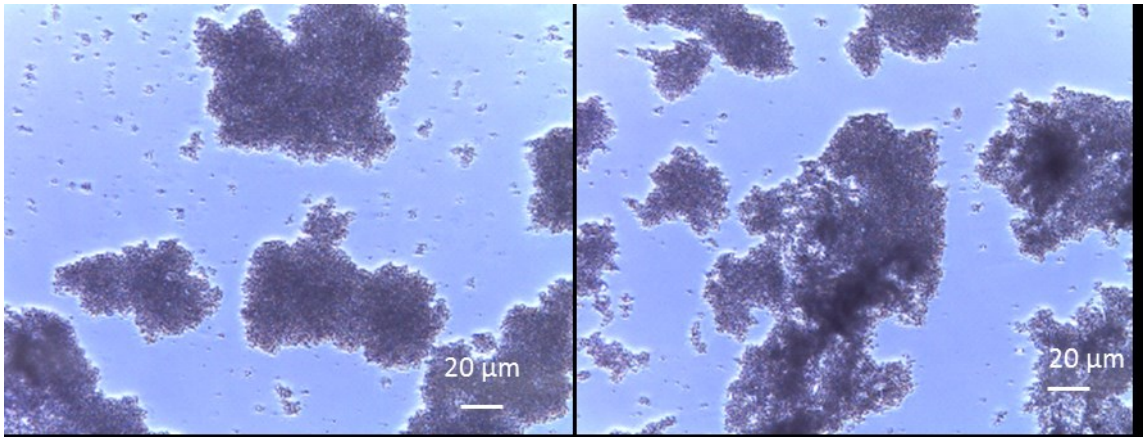

(a) with 1 w/w% CH_3COOH solution (b) with 5 w/w% CH_3COOH solution

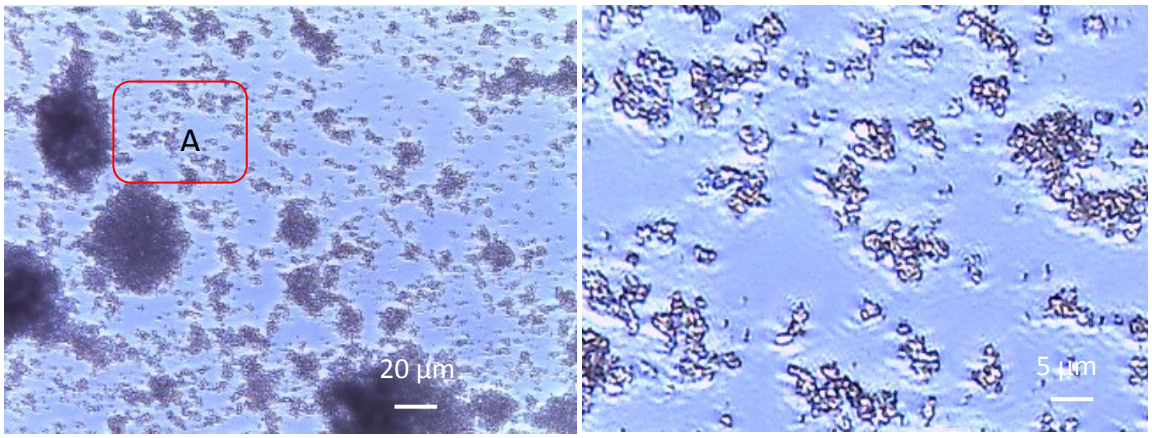

(c) with 10 w/w% CH_3COOH solution (d) Region A in (c) magnified

Fig. 18 Microscopic images for the sample of MNFC:DGCC 3:7 with artificial acidification achieved by adding CH_3COOH: (a) adding 1 w/w% solution concentration, (b) adding 5 w/w% solution concentration, (c) adding 10 w/w% solution concentration, and (d) an enlarged image of Region A showing the effect of acid shock flocculating and then aggregating the GCC particles before they can heterogeneously flocculate with the cellulose, resulting in size exclusion.

The action of direct weak acid addition, therefore, fails to promote adsorption onto the nanofibrils and this supports the finding that the bulk pH drift downwards over time is not the prime driving force for adsorption, but rather the material interface action of the localised H_3O^+ together with sufficient induced dwell time of contact.

4. Conclusions

In this paper, we discussed the use of ultrafine calcium carbonate nano particles to probe the surface reactivity of nanofibrils as found in micro nanofibrillated cellulose (MNFC), derived from earlier findings regarding the dewatering mechanism of aqueous MNFC gel materials by adding colloidally unstable mineral particles, such as undispersed calcium carbonate. Firstly, the observation that application of ultralow shear (0.01 s^{-1}) over extended time scales leads to structuration and eventual dewatering was confirmed using undispersed ground calcium carbonate (UGCC). To establish the mechanism of interaction between the carbonate and the nanofibril surface, a further sample of polyacrylate dispersed calcium carbonate (DGCC) was used for comparison, and initially the resistance to structuration and dewatering, also found earlier, was confirmed, however newly it was found that by cycling the application of ultralow shear with storage periods between led, after extended times of many days, to eventual structuration and dewatering.

We conclude that the surface bound water on the nanofibril surface, when brought into contact with the otherwise mobile GCC particles by action of applying ultralow shear rate, activates the carbonate surface by a mechanism of weak acid and conjugate base equilibrium, such that locally dissociated Ca^{2+} ion forms an insoluble salt bridge to the nanofibril surface. This mechanism is shown to contrast with induced particle flocculation by increased conductivity resulting from addition of free Ca^{2+}, which, rather than causing particle adsorption onto the nanofibrils, leads instead to autoflocculation of the mineral particles. Furthermore, by adding weak acid to the mixed suspension heterogeneous flocculation is immediately promoted, however excess acid results in colloidal shock and a large proportion of the particles are agglomerated prior to adsorption and so remain in the water phase due to size exclusion from the surface.

That the surface adsorbed restrained water on the nanofibrils undergoes hydrogen bonding supports the likelihood of there being an equilibrium H_3O^+ dissociation on the fibril surface, and this can be shown, as we believe, for the first time using nanoparticles of calcium carbonate as a probe

Acknowledgements

The work was solely supported financially by Omya International AG, Switzerland.

References

1. Herrick, F.W., Casebier, R.L., Hamilton, J.K., Sandberg, K.R., Microfibrillated cellulose: morphology and accessibility, J. Appl. Polym. Sci.: Appl. Polym. Symp; (United States), Vol. 37, No. CONF-8205234-Vol. 2 (1983), ITT Rayonier Inc., Shelton, WA.

2. Spence, K.L., Venditti, R.A., Rojas, O.J., Habibi, Y., Pawlak, J.J., A comparative study of energy consumption and physical properties of microfibrillated cellulose produced by different processing methods, Cellulose , 18(4) (2011), pp 1097-1111.

3. Schenker, M., Schoelkopf, J., Mangin, P., Gane. P.A.C. , Pigmented micro-nanofibrillated cellulose (MNFC) as packaging composite material: a first assessment. In: Proceedings of the Tappi PaperCon 2015, (2015) Conference, Atlanta, Tappi Press, Atlanta.

4. Schenker, M., Schoelkopf, J., Mangin, P., Gane. P.A.C., Rheological investigation of complex micro and nanofibrillated cellulose (MNFC) suspensions: discussion of flow curves and gel stability. Tappi J. 15 (2016), pp 405–416.

5. Nazari, B., Moghaddam, R.H., Bousfield, D., A three dimensional model of a vane rheometer. Int. J. Heat Fluid Flow, 42 (2013), pp 289–295.

6. Puisto, A., Illa, X., Mohtaschemi, M., Alava, M., Modeling the rheology of nanocellulose suspensions. Nordic Pulp and Paper Res. J., 27(2) (2012), pp 277-281.

7. Dimic-Misic, K., Puisto, A., Paltakari, J., Alava, M., Maloney, T., The influence of shear on the dewatering of high consistency nanofibrillated cellulose furnishes. Cellulose 20 (4) (2013), pp 1853–1864.

8. Dimic-Misic, K., Puisto, A., Gane, P.A.C., Nieminen, K., Alava, M., Paltakari, J., Maloney, T., The role of MFC/NFC swelling in the rheological behavior and dewatering of high consistency furnishes. Cellulose 20(6) (2013), pp 2847–28617.

9. Dimic-Misic, K., Maloney, T., Liu, G., Gane, P.A.C., Micro nanofibrillated cellulose (MNFC) gel dewatering induced at ultralow-shear in presence of added colloidally-unstable particles. Cellulose 24(3) (2017), pp 1463–1481.

10. Hatakeyama, T., Hatakeyama, H., Heat capacity and nuclear magnetic relaxation times of non-freezing water restrained by polysaccharides, revisited. Journal of Biomaterials Science, Polymer Edition, (2017), Taylor and Francis online, DOI: 10.1080/09205063.2017.1291551.

11. Hatakeyama, T., Inui, Y., Iijima, M., Hatakeyama, H., Bound water restrained by nanocellulose fibres. Journal of Thermal Analysis and Calorimetry, 113(3) (2013), pp 1019–1025.

12. Dimic-Misic, K., Rantanen, J., Maloney, T.C., Gane, P.A.C., Gel structure phase behavior in micro nanofibrillated cellulose containing *in-situ* precipitated calcium carbonate. J Appl. Polym. Sci., 132(22), (2016), pp43486.

13. Maloney, T., Network swelling of TEMPO-oxidized nanocellulose, Holzforschung, 69(2) (2015), pp 207-213.

14. Shen, J., Song, Z., Qian, X., Zhan, Y., Method for the preparation of acid-tolerant calcium carbonate fillers and filled paper based on high-lignin-content deinked pulp derived from recycled newspaper. Patent US 20120111520 A1, 2012. 5.10.

15. Passaretti, J.D., Acid-stabilized calcium carbonate, process for its production and method for its use in the manufacture of acidic paper, Patent US 5043017 A, 1991.

16. Derjaguin, B., Landau, L., Theory of the stability of strongly charged lyophobic sols and of the adhesion of strongly charged particles in solutions of electrolytes.Progress in surface science,43(1-4)(1993),30-59.

17. Verwey, E.J.W., Overbeek, J.Th.G., Theory of the stability of lyophobic colloids. Publishing company, INC ,1948.